Semi-Emperical Calculation of the Transport Properties of Eight Binary Gas Mixtures at Low Density by the Inversion Method

Mohammad Mehdi Papari* **and Ali Boushehri**

Department of Chemistry, Shiraz University, Shiraz 71454, Iran

(Received March 27, 1998)

Viscosities, diffusion coefficients, and thermal-diffusion factors for eight equimolar binary gas mixtures ($Ne+O_2$, $Ne+CO_2$, $Ne+N_2O$, $Ne+SF_6$, $Ar+O_2$, $Ar+CO_2$, $Ar+N_2O$, and $Ar+SF_6$) were determined based on the principle of the corresponding states of viscosity using the inversion technique. The Lennard-Jones 12-6 potential energy function was used as the initial model potential required by the technique. Typically, the interaction potential of $Ar+SF_6$ has been compared with those obtained from thermal-diffusion measurements. Our inverted potentials are in excellent agreement with it. The interaction potential energies from the inversion procedure reproduce the viscosities to within 1%, the diffusion coefficients to within 5%, and the thermal-diffusion factors to within 25%.

The central problem in molecular physics is how to calculate the intermolecular potential energy. However, no direct way to measure the intermolecular potential energy is known, and what is generally available are measurements of some macroscopically observable quantity having some functional dependence on the intermolecular forces. The problem is, thus, how to extract information about these forces by analyzing the measurements. Every macroscopic property, which has two very restrictive conditions, is suitable for obtaining the potential energy. These are: 1) an accurate statistical mechanical theory connecting the intermolecular forces and the macroscopic properties must be available, 2) the forces must not be buried under too many layers of theory. In this respect, the traditional approach for establishing the nature of the potential energy between molecules from the macroscopic properties is to introduce some mathematical form for the potential energy and, then, to determine the parameters of the model by comparing the calculated macroscopic properties with the experiments.[1] However, this procedure does not produce a unique potential; another major problem here is that, as the number of adjustable parameters increases, difficulties for fixing them with experiments arise. This restriction persuaded the investigators to introduce a numerical technique, known as the inversion procedure. This procedure, in an iterative form, was put forward by Smith and co-workers.[2—4] The main advantages of this approach are that it produces a unique potential and also removes any lengthy multiparameter fitting procedure, outlined in traditional approach. Recently, the inversion procedure has also been successfully applied to transport and equilibrium data and their corresponding state correlations by Boushehri et al.[5—12]

Our inversion method is closely based on those of the Smith method of the inversion procedure. This method will be explained in detail in the next sections.

In addition to the inversion of bulk properties, there are other sources for obtaining intermolecular forces. These are: 1) quantum mechanical calculations (ab initio method), 2) molecular-beam scattering, and 3) spectroscopic observations. In this work we restricted ourselves to the extraction of information about the intermolecular potential energy from the transport properties. In this respect, according to kinetic theory of gases at low density and the Chapman–Enskog solution of the Boltzman equation, the transport properties can be expressed based on a series of collision integrals that depend on the intermolecular potential energy, and is defined as

$$\theta = \pi - 2b\int_{r_0}^{\infty} \frac{r^{-2}\mathrm{d}r}{\{1-(b^2/r^2)-(V(r)/E)\}^{1/2}}, \tag{1}$$

$$Q^{(l)}(E) = 2\pi\left[1-\frac{1+(-1)^l}{2(1+l)}\right]^{-1}\int_0^{\infty}(1-\mathrm{Cos}^l\,\theta)b\mathrm{d}b, \tag{2}$$

$$\Omega^{(l,s)}(T) = [(s+1)!(kT)^{s+2}]^{-1}\int_0^{\infty} Q^{(l)}(E)\exp(-E/kT)E^{s+1}\mathrm{d}E, \tag{3}$$

where θ is the scattering angle, $Q^{(l)}(E)$ the transport collision integral, b the impact parameter, E the relative kinetic energy of colliding molecules and r_0 the closest approach of two molecules; kT has its usual meaning. Thus, three successive numerical integrations are required to obtain a collision integral. Numerical differentiation and use of the recursion relation can generate collision integrals higher than that mentioned,

$$\Omega^{*(l,s+1)} = \Omega^{*(l,s)}\left[1+\frac{1}{s+2}\frac{\mathrm{d}\ln\Omega^{*(l,s)}}{\mathrm{d}\ln T}\right], \tag{4}$$

where the reduced collision integral is defined by

$$\Omega^{*(l,s)} = \frac{\Omega^{(l,s)}}{\pi\sigma^2}, \tag{5}$$

and σ is length scaling factor, such that $V(\sigma) = 0$. It must be mentioned that since $V(r)$, in our work, is defined such that $V(\sigma_0) = 0$, it turns out that σ_0 is nearly equal to σ; more precisely, $\sigma_0/\sigma = 0.997$. Higher collision integrals are defined in Ref. 13.

The potential energy would serve as the input information required in calculating the collision integrals, and consequently the transport properties. Kinetic-theory expressions for the transport properties in term of the collision integrals for pure gases and a mixture of gases are given in the following sections.

In the present work, the vicosities, diffusion coefficients, and thermal-diffusion factors for eight equimolar and low-density binary gas mixtures ($Ne+O_2$, $Ne+CO_2$, $Ne+N_2O$, $Ne+SF_6$, $Ar+O_2$, $Ar+CO_2$, $Ar+N_2O$, and $Ar+SF_6$) were calculated based on the extended law of the corresponding states using the inversion method. Our accuracies are within 1% for the viscosities, 5% for the diffusion coefficients, and 25% for the thermal-diffusion factors. It is of interest to note that excellent agreement between the interaction potential obtained by the inversion method and that obtained by Taylor et al.[14] has been obtained.

There exist a voracious need in industry for reliable data on the thermophysical properties of a very large set of pure substances, and an even larger set of mixtures of all kinds. The number of systems is so large that direct experimental measurements on all of them is out of the question, and a maximum input from theory is required. The tables of numerical data are not meant to be exhaustive, and were not designed for linear interpolation. They are convenient extracts only, because the algorithm for each property can be programmed on a computer based on the information supplied here. We do not yet include the explicit effects of the internal degrees of freedom on the transport properties, which rules out a calculation of the thermal conductivity. An additional 7 figures have been deposited with the principle author and may be supplied upon the request of readers.

Extended Principle of Corresponding States

The law of corresponding states rest on this idea that the equilibrium and transport properties of substances whose molecules obey a potential function with two scaling parameters, (ε, energy scaling factor and σ, length scaling factor) can be expressed in terms of functions that are nearly universal when written in terms of scaling factors. Earlier work on the viscosity of the noble gases showed that the function $\Omega^{*(2,2)}$ is universal among the monatomic gases.[15] Work concerning the viscosity of binary gas mixtures also strongly indicates that a similar principle could be applied.[16,17]

The extended law of corresponding states is a revised principle of corresponding states that characterises each binary interaction with the aid of five scaling parameters instead of two. The five scaling parameters are σ, ε, ρ^*, C_6^*, V_0^*; also, a single quantum mechanical parameter, Λ^*, maybe come into play. A dimensionless parameter, C_6^*, characterises the long-range region of the potential-energy curve (low temperature), and the dimensionless parameters ρ^* and V_0^* characterise the short-range region repulsive wall (for further discussion see Ref. 18). The quantum mechanical parameter Λ^* become significant when molecular partners are small and/or the temperature is low.

In our work the functional correlation obtained from an extended law of corresponding states of viscosity using the inversion method in order to calculate the unlike-pair potential energy was applied. These correlation equations, which have been taken from Bzowski et al.,[19] are as follows:

Viscosity Collision Integrals, $\Omega^{*(2,2)}$ for Molecular Gases.

a) $1 \leq T^* \leq 10$

$$\Omega^{*(2,2)} = \exp[0.46641 - 0.56991(\ln T^*) + 0.19591(\ln T^*)^2 - 0.03879(\ln T^*)^3 + 0.00259(\ln T^*)^4], \quad (6)$$

where $T^* = kT/\varepsilon$.

b) $T^* \geq 10$

$$\Omega^{*(2,2)} = (\rho^*)^2\alpha^2[1.04 + a_1(\ln T^*)^{-1} + a_2(\ln T^*)^{-2} + a_3(\ln T^*)^{-3} + a_4(\ln T^*)^{-4}], \quad (7)$$

where

$$a_1 = 0, \quad (7a)$$

$$a_2 = -33.0838 + (\alpha_{10}\rho^*)^{-2}[20.0862 + (72.1059/\alpha_{10}) + (8.27648/\alpha_{10})^2], \quad (7b)$$

$$a_3 = 101.5710 - (\alpha_{10}\rho^*)^{-2}[56.4472 + (286.3930/\alpha_{10}) + (17.7610/\alpha_{10})^2], \quad (7c)$$

$$a_4 = -87.7036 + (\alpha_{10}\rho^*)^{-2}[46.3130 + (277.1460/\alpha_{10}) + (19.0573/\alpha_{10})^2]. \quad (7d)$$

In the above relations $\alpha_{10} = \ln(V_0^*/10)$ is the value of $\alpha = \ln V_0^* - \ln T^*$ at the matching point of $T^* = 10$.

Viscosity Collision Integral, $\Omega^{*(2,2)}$, for Noble Gases.

a) $T^* \leq 1.2$

$$\Omega^{*(2,2)} = 1.1943(C_6^*/T^*)^{1/3}[1 + a_1(T^*)^{1/3} + a_2(T^*)^{2/3} + a_3(T^*) + a_4(T^*)^{4/3} + a_5(T^*)^{5/3} + a_6(T^*)^2], \quad (8)$$

where

$$a_1 = 0.18, \quad (8a)$$

$$a_2 = 0, \quad (8b)$$

$$a_3 = -1.20407 - 0.195866(C_6^*)^{-1/3}, \quad (8c)$$

$$a_4 = -9.86374 + 20.2221(C_6^*)^{-1/3}, \quad (8d)$$

$$a_5 = 16.6295 - 31.3613(C_6^*)^{-1/3}, \quad (8e)$$

$$a_6 = -6.73805 + 12.6611(C_6^*)^{-1/3}. \quad (8f)$$

b) $1.2 \leq T^* \leq 10$

$\Omega^{*(2,2)}$ = The same as Eq. 6.

c) $T^* \geq 10$

$\Omega^{*(2,2)}$ = The same as Eq. 7.

Inversion Procedure. Given a set of experimental reduced viscosity collision integrals, $\Omega^{*(2,2)}$, over a wide-

range region of temperatures from Eqs. 6, 7, and 8 and the initial potential model, it is possible to invert a pair of values ($\Omega^{*(2,2)}$, T) to V/ε as a function of r/σ using the relations

$$r^* = r/\sigma = (\Omega^{*(2,2)})^{1/2}, \tag{9}$$

$$V^* = V/\varepsilon = GT^*. \tag{10}$$

The inversion function (G) is a function of the reduced temperature (T^*) alone in a complicated way, and may be calculated using a model system whose intermolecular potential-energy function is known. Accordingly, the values of G for the Lennard–Jones 12-6 (LJ 12-6) model potential, as the initial model, has been determined from Viehland et al.[20] The new potential energies are closer approximations to the true potential than the potential of the initial model. The new potential, then, can be applied to calculations of improved collision integrals by using the integrals in Eqs. 1, 2, and 3 of the Gatland version of the computer program developed by O'Hara and Smith.[21,22] This process is repeated until convergence occurs. The convergence condition is the degree to which the calculated collision integrals for a given iteration are close to the experimental correlation within experimental accuracy.[2]

It should be mentioned that the rate of convergence of iteration reflects the differences of detail between the initial potential and the potential obtained around an iteration. In general, of course, the closer is two potentials functions, the faster is the convergence.[23]

The present results which we have obtained converged after two iterations, and the results are given in the next section.

Results and Discussion

As mentioned before, the problem of obtaining the interaction potential energy is the extraction of information about the forces by analyzing the bulk properties. The degree of success will depend on the accuracy of both the measurements and theory connecting the forces to macroscopic properties, and on the sensitivity of this connection. The transport coefficients of dilute gases, especially viscosity, which depends on the binary interactions, satisfy the above conditions. In this respect, the inversion procedure plays an important role for generating an unlike-molecule potential from the viscosity data and their corresponding states correlations. This, in turn, permits us to calculate collision integrals, and, consequently, the transport properties more accurately than is possible by correlations of the corresponding states.

In the case of the corrsponding states principle, it must be mentioned that since the functional equations obtained from this principle apply in a more limited form to molecular gases than to noble gases, the arithmetic mean of the functions should be used for gases 1 and 2. Also, we are confined only to $T^* \geq 1.0$, because viscosity collision integrals for molecular gases at low temperature do not exist (see Ref. 24); consequently, in order to proceed to the next iteration it is necessary to extrapolate $V(r)$ at the long-range region (low temperature). The extrapolation function that we have used is $V^* = -C_6u^6$, where C_6 is the dispersion coefficient and u is the reciprocal of the intermolecular distances, both in atomic units. It is remarkable to mention that the inversion procedure is insensitive to the nature of the extrapolating function.[2]

In the present work we obtained accurate reduced potential energies for eight equimolar binary gas mixtures at low density by direct inversion of the viscosity collision integral equations. The results for the Ar+SF_6 system are shown in Fig. 1, and compared with the potential energies obtained by Taylor and his co-worker.[14] These accurate potential energies have produced improved collision integrals. The results of collision integrals and their ratios are given in Tables 1, 2, 3, 4, 5, 6, 7, and 8. The ratios of the calculated collision integrals have been determined by the following equations:

$$A^* = \frac{\Omega^{*(2,2)}}{\Omega^{*(1,1)}}, \tag{11}$$

$$B^* = \frac{\left[5\Omega^{*(1,2)} - 4\Omega^{*(1,3)}\right]}{\Omega^{*(1,1)}}, \tag{12}$$

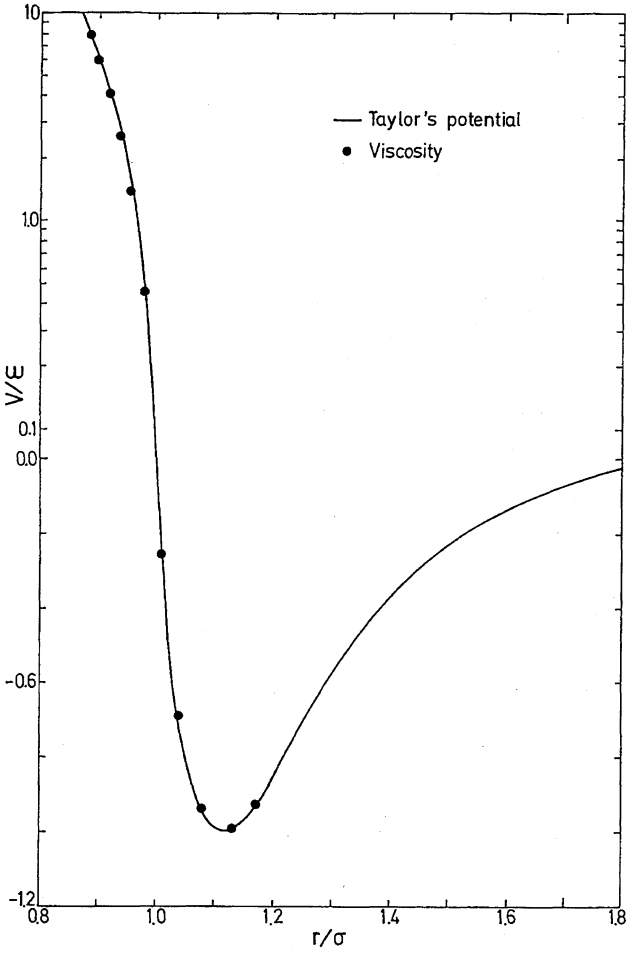

Fig. 1. The reduced pair potential energy for Ar+SF_6 system. The results of inversion of viscosity data shown by ●. The solid line, shown for comparison, is Taylor's potential.[14]

Table 1. The Reduced Collision Integrals and Their Ratios for $Ne+O_2$ System

$\log T^*$	$\Omega^{*(1,1)}$	$\Omega^{*(2,2)}$	A^*	B^*	C^*	E^*	F^*
0.0	1.3977	1.5527	1.1109	1.1956	0.8482	0.8820	0.9221
0.1	1.2629	1.3969	1.1061	1.1676	0.8591	0.8893	0.9290
0.2	1.1511	1.2677	1.1013	1.1438	0.8727	0.9005	0.9384
0.3	1.0594	1.1635	1.0982	1.1256	0.8872	0.9133	0.9493
0.4	0.9847	1.0805	1.0973	1.1129	0.9009	0.9258	0.9608
0.5	0.9234	1.0142	1.0984	1.1049	0.9127	0.9365	0.9718
0.6	0.8724	0.9605	1.1010	1.1003	0.9224	0.9449	0.9817
0.7	0.8290	0.9157	1.1045	1.0981	0.9298	0.9511	0.9902
0.8	0.7913	0.8772	1.1086	1.0973	0.9352	0.9554	0.9972
0.9	0.7577	0.8432	0.1128	1.0976	0.9390	0.9584	1.0027
1.0	0.7271	0.8123	1.1171	1.0991	0.9414	0.9605	1.0069
1.1	0.6986	0.7838	1.1220	1.1023	0.9426	0.9620	1.0098
1.2	0.6715	0.7572	1.1276	1.1069	0.9427	0.9628	1.0121
1.3	0.6453	0.7316	1.1338	1.1113	0.9418	0.9621	1.0148
1.4	0.6196	0.7057	1.1390	1.1121	0.9407	0.9592	1.0186
1.5	0.5946	0.6783	1.1407	1.1062	0.9404	0.9544	1.0236
1.6	0.5709	0.6488	1.1365	1.0928	0.9421	0.9493	1.0285
1.7	0.5492	0.6181	1.1255	1.0735	0.9465	0.9460	1.0316
1.8	0.5305	0.5881	1.1085	1.0519	0.9535	0.9463	1.0321
1.9	0.5152	0.5606	1.0881	1.0317	0.9621	0.9506	1.0299
2.0	0.5035	0.5374	1.0673	1.0152	0.9714	0.9580	1.0260

Table 2. The Reduced Collision Integrals and Their Ratios for $Ne+CO_2$ System

$\log T^*$	$\Omega^{*(1,1)}$	$\Omega^{*(2,2)}$	A^*	B^*	C^*	E^*	F^*
0.0	1.4004	1.5557	1.1109	1.1963	0.8483	0.8825	0.9221
0.1	1.2655	1.4001	1.1064	1.1685	0.8591	0.8896	0.9290
0.2	1.1533	1.2709	1.1020	1.1448	0.8725	0.9006	0.9384
0.3	1.0612	1.1664	1.0990	1.1265	0.8868	0.9131	0.9495
0.4	0.9861	1.0828	1.0980	1.1133	0.9004	0.9252	0.9611
0.5	0.9245	1.0157	1.0987	1.1043	0.9125	0.9356	0.9723
0.6	0.8733	0.9610	1.1004	1.0984	0.9224	0.9439	0.9824
0.7	0.8301	0.9153	1.1027	1.0944	0.9304	0.9501	0.9909
0.8	0.7929	0.8762	1.1051	1.0919	0.9365	0.9547	0.9978
0.9	0.7601	0.8418	1.1075	1.0905	0.9411	0.9582	1.0032
1.0	0.7307	0.8110	1.1100	1.0905	0.9444	0.9609	1.0070
1.1	0.7036	0.7832	1.1131	1.0923	0.9464	0.9633	1.0097
1.2	0.6783	0.7578	1.1172	1.0957	0.9473	0.9649	1.0117
1.3	0.6541	0.7339	1.1220	1.0992	0.9472	0.9651	1.0141
1.4	0.6305	0.7102	1.1263	1.0998	0.9467	0.9631	1.0176
1.5	0.6077	0.6853	1.1276	1.0945	0.9468	0.9592	1.0222
1.6	0.5861	0.6586	1.1238	1.0826	0.9486	0.9548	1.0269
1.7	0.5664	0.6308	1.1138	1.0654	0.9526	0.9519	1.0299
1.8	0.5492	0.6034	1.0985	1.0462	0.9589	0.9521	1.0305
1.9	0.5353	0.5781	1.0801	1.0282	0.9666	0.9558	1.0285
2.0	0.5245	0.5567	1.0613	1.0135	0.9748	0.9624	1.0249

Table 3. The Reduced Collision Integrals and Their Ratios for $Ne+N_2O$ System

$\log T^*$	$\Omega^{*(1,1)}$	$\Omega^{*(2,2)}$	A^*	B^*	C^*	E^*	F^*
0.0	1.4032	1.5615	1.1129	1.1971	0.8477	0.8820	0.9228
0.1	1.2674	1.4046	1.1083	1.1692	0.8584	0.8889	0.9297
0.2	1.1545	1.2741	1.1036	1.1452	0.8719	0.8999	0.9391
0.3	1.0620	1.1686	1.1004	1.1267	0.8863	0.9124	0.9501
0.4	0.9865	1.0842	1.0991	1.1134	0.9000	0.9246	0.9616
0.5	0.9246	1.0616	1.0995	1.1044	0.9122	0.9352	0.9727
0.6	0.8733	0.9615	1.1010	1.0985	0.9222	0.9436	0.9826
0.7	0.8299	0.9156	1.1032	1.0947	0.9302	0.9499	0.9910
0.8	0.7926	0.8763	1.1056	1.0923	0.9363	0.9546	0.9979
0.9	0.7597	0.8419	1.1081	1.0911	0.9409	0.9581	1.0032
1.0	0.7302	0.8111	1.1108	1.0913	0.9441	0.9609	1.0071
1.1	0.7030	0.7832	1.1140	1.0932	0.9461	0.9632	1.0097
1.2	0.6776	0.7577	1.1182	1.0968	0.9469	0.9647	1.0118
1.3	0.6531	0.7336	1.1232	1.1004	0.9467	0.9649	1.0141
1.4	0.6294	0.7097	1.1276	1.1011	0.9461	0.9628	1.0177
1.5	0.6063	0.6846	1.1290	1.0958	0.9462	0.9587	1.0224
1.6	0.5845	0.6576	1.1152	1.0837	0.9479	0.9542	1.0271
1.7	0.5645	0.6295	1.1151	1.0663	0.9520	0.9513	1.0302
1.8	0.5472	0.6018	1.0997	1.0468	0.9583	0.9515	1.0307
1.9	0.5331	0.5763	1.0811	1.0286	0.9661	0.9552	1.0287
2.0	0.5222	0.5546	1.0620	1.0137	0.9744	0.9619	1.0250

Table 4. The Reduced Collision Integrals and Their Ratios for $Ne+SF_6$ System

$\log T^*$	$\Omega^{*(1,1)}$	$\Omega^{*(2,2)}$	A^*	B^*	C^*	E^*	F^*
0.0	1.4026	1.5685	1.1183	1.1965	0.8488	0.8808	0.9238
0.1	1.2678	1.4096	1.1118	1.1693	0.8593	0.8881	0.9306
0.2	1.1555	1.2779	1.1060	1.1457	0.8725	0.8993	0.9398
0.3	1.0633	1.1715	1.1018	1.1272	0.8867	0.9120	0.9505
0.4	0.9879	1.0865	1.0999	1.1137	0.9002	0.9242	0.9620
0.5	0.9260	1.0183	1.0997	1.1041	0.9123	0.9346	0.9731
0.6	0.8747	0.9626	1.1005	1.0972	0.9225	0.9429	0.9831
0.7	0.8315	0.9161	1.1017	1.0920	0.9308	0.9492	0.9916
0.8	0.7946	0.8763	1.1029	1.0880	0.9374	0.9540	0.9985
0.9	0.7623	0.8414	1.1037	1.0850	0.9426	0.9597	1.0038
1.0	0.7338	0.8105	1.1045	1.0831	0.9467	0.9608	1.0077
1.1	0.7080	0.7828	1.1056	1.0828	0.9496	0.9635	1.0103
1.2	0.6842	0.7577	1.1074	1.0839	0.9515	0.9658	1.0121
1.3	0.6619	0.7346	1.1099	1.0852	0.9525	0.9668	1.0142
1.4	0.6407	0.7124	1.1119	1.0844	0.9531	0.9661	1.0171
1.5	0.6204	0.6895	1.1118	1.0791	0.9541	0.9636	1.0210
1.6	0.6015	0.6661	1.1075	1.0684	0.9564	0.9606	1.0250
1.7	0.5844	0.6417	1.0982	1.0537	0.9603	0.9587	1.0280
1.8	0.5696	0.6178	1.0847	1.0376	0.9659	0.9593	1.0280
1.9	0.5576	0.5959	1.0687	1.0226	0.9726	0.9670	1.0262
2.0	0.5484	0.5772	1.0524	1.0104	0.9795	0.9683	1.0228

Table 5. The Reduced Collision Integrals and Their Ratios for Ar+O_2 System

$\log T^*$	$\Omega^{*(1,1)}$	$\Omega^{*(2,2)}$	A^*	B^*	C^*	E^*	F^*
0.0	1.3995	1.5586	1.1137	1.1961	0.8475	0.8811	0.9230
0.1	1.2640	1.4012	1.1085	1.1678	0.8585	0.8884	0.9301
0.2	1.1516	1.2706	1.1033	1.1438	0.8723	0.8996	0.9394
0.3	1.0597	1.1653	1.0997	1.1256	0.8868	0.9126	0.9501
0.4	0.9847	1.0815	1.0983	1.1131	0.9006	0.9252	0.9613
0.5	0.9232	1.0148	1.0992	1.1054	0.9125	0.9362	0.9720
0.6	0.8720	0.9609	1.1019	1.1014	0.9220	0.9449	0.9816
0.7	0.8284	0.9162	1.1059	1.0999	0.9293	0.9513	0.9899
0.8	0.7904	0.8778	1.1106	1.1000	0.9344	0.9556	0.9969
0.9	0.7563	0.8438	1.1156	1.1013	0.9378	0.9584	1.0024
1.0	0.7251	0.8128	1.1210	1.1039	0.9398	0.9602	1.0067
1.1	0.6958	0.7840	1.1268	1.1080	0.9405	0.9614	1.0097
1.2	0.6677	0.7568	1.1335	1.1136	0.9400	0.9618	1.0122
1.3	0.6403	0.7303	1.1406	1.1186	0.9387	0.9606	1.0150
1.4	0.6133	0.7033	1.1466	1.1198	0.9371	0.9571	1.0191
1.5	0.5871	0.6744	1.1487	1.1138	0.9364	0.9516	1.0243
1.6	0.5621	0.6432	1.1445	1.0995	0.9380	0.9459	1.0293
1.7	0.5392	0.6109	1.1328	1.0789	0.9425	0.9424	1.0325
1.8	0.5195	0.5792	1.1149	1.0559	0.9499	0.9427	1.0329
1.9	0.5034	0.5503	1.0933	1.0342	0.9591	0.9472	1.0307
2.0	0.4910	0.5260	1.0713	1.0165	0.9690	0.9551	1.0267

Table 6. The Reduced Collision Integrals and Their Ratios for Ar+CO_2 System

$\log T^*$	$\Omega^{*(1,1)}$	$\Omega^{*(2,2)}$	A^*	B^*	C^*	E^*	F^*
0.0	1.4008	1.5596	1.1133	1.1965	0.8475	0.8815	0.9228
0.1	1.2653	1.4023	1.1083	1.1683	0.8584	0.8886	0.9299
0.2	1.1527	1.2718	1.1033	1.1444	0.8721	0.8997	0.9392
0.3	1.0605	1.1664	1.0999	1.1260	0.8866	0.9125	0.9501
0.4	0.9853	1.0824	1.0985	1.1131	0.9004	0.9250	0.9614
0.5	0.9237	1.0154	1.0993	1.1049	0.9124	0.9358	0.9723
0.6	0.8724	0.9610	1.1015	1.1002	0.9221	0.9444	0.9820
0.7	0.8290	0.9159	1.1048	1.0978	0.9297	0.9508	0.9904
0.8	0.7913	0.8772	1.1086	1.0969	0.9352	0.9552	0.9973
0.9	0.7577	0.8430	1.1126	1.0972	0.9391	0.9583	1.0027
1.0	0.7271	0.8121	1.1169	1.0988	0.9415	0.9605	1.0068
1.1	0.6987	0.7837	1.1217	1.1021	0.9428	0.9621	1.0097
1.2	0.6716	0.7572	1.1274	1.1069	0.9428	0.9630	1.0120
1.3	0.6454	0.7317	1.1337	1.1114	0.9419	0.9623	1.0147
1.4	0.6197	0.7059	1.1391	1.1124	0.9407	0.9594	1.0186
1.5	0.5947	0.6786	1.1410	1.1067	0.9403	0.9545	1.0236
1.6	0.5709	0.6491	1.1369	1.0933	0.9420	0.9493	1.0285
1.7	0.5492	0.6184	1.1259	1.0739	0.9463	0.9459	1.0317
1.8	0.5304	0.5882	1.1090	1.0523	0.9532	0.9461	1.0321
1.9	0.5151	0.5607	1.0886	1.0320	0.9619	0.9504	1.0300
2.0	0.5033	0.5374	1.0677	1.0154	0.9712	0.9578	1.0261

$$C^* = \frac{\Omega^{*(1,2)}}{\Omega^{*(1,1)}}, \tag{13}$$

$$E^* = \frac{\Omega^{*(2,3)}}{\Omega^{*(2,2)}}, \tag{14}$$

$$F^* = \frac{\Omega^{*(3,3)}}{\Omega^{*(1,1)}}. \tag{15}$$

Table 7. The Reduced Collision Integrals and Their Ratios for Ar+N_2O System

$\log T^*$	$\Omega^{*(1,1)}$	$\Omega^{*(2,2)}$	A^*	B^*	C^*	E^*	F^*
0.0	1.3978	1.5531	1.1112	1.1956	0.8481	0.8819	0.9221
0.1	1.2630	1.3972	1.1063	1.1677	0.8591	0.8892	0.9290
0.2	1.1511	1.2680	1.1015	1.1439	0.8727	0.9004	0.9384
0.3	1.0595	1.1637	1.0984	1.1256	0.8871	0.9133	0.9493
0.4	0.9847	1.0806	1.0974	1.1129	0.9008	0.9257	0.9609
0.5	0.9233	1.0142	1.0984	1.1048	0.9127	0.9363	0.9719
0.6	0.8723	0.9603	1.1009	1.1000	0.9224	0.9448	0.9818
0.7	0.8290	0.9155	1.1043	1.0976	0.9299	0.9510	0.9903
0.8	0.7914	0.8770	1.1082	1.0967	0.9354	0.9554	0.9972
0.9	0.7579	0.8429	1.1122	1.0969	0.9393	0.9584	1.0027
1.0	0.7274	0.8121	1.1165	1.0985	0.9417	0.9606	1.0068
1.1	0.6991	0.7838	1.1213	1.1017	0.9430	0.9611	1.0097
1.2	0.6721	0.7574	1.1270	1.1065	0.9430	0.9632	1.0119
1.3	0.6459	0.7320	1.1333	1.1110	0.9421	0.9625	1.0146
1.4	0.6203	0.7064	1.1387	1.1121	0.9409	0.9596	1.0850
1.5	0.5954	0.6791	1.1406	1.1064	0.9405	0.9547	1.0235
1.6	0.5717	0.6497	1.1366	1.0931	0.9422	0.9495	1.0284
1.7	0.5500	0.6191	1.1256	1.0738	0.9465	0.9461	1.0316
1.8	0.5312	0.5890	1.1087	1.0523	0.9534	0.9463	1.0321
1.9	0.5159	0.5615	1.0884	1.0320	0.9620	0.9505	1.0299
2.0	0.5041	0.5382	1.0676	1.0154	0.9712	0.9579	1.0261

Table 8. The Reduced Collision Integrals and Their Ratios for Ar+SF_6 System

$\log T^*$	$\Omega^{*(1,1)}$	$\Omega^{*(2,2)}$	A^*	B^*	C^*	E^*	F^*
0.0	1.4007	1.5588	1.1128	1.1960	0.8488	0.8821	0.9222
0.1	1.2662	1.4025	1.1077	1.1685	0.8594	0.8893	0.9292
0.2	1.1542	1.2728	1.1028	1.1451	0.8727	0.9004	0.9385
0.3	1.0622	1.1679	1.0995	1.1268	0.8869	0.9129	0.9495
0.4	0.9871	1.0840	1.0982	1.1136	0.9005	0.9250	0.9610
0.5	0.9254	1.0167	1.0987	1.1044	0.9125	0.9354	0.9722
0.6	0.8742	0.9618	1.1003	1.0982	0.9224	0.9437	0.9823
0.7	0.8309	0.9159	1.1023	1.0939	0.9305	0.9499	0.9909
0.8	0.7937	0.8765	1.1044	1.0907	0.9367	0.9545	0.9980
0.9	0.7611	0.8419	1.1062	1.0886	0.9416	0.9579	1.0034
1.0	0.7319	0.8110	1.1081	1.0877	0.9451	0.9607	1.0074
1.1	0.7053	0.7831	1.1102	1.0882	0.9476	0.9631	1.0101
1.2	0.6806	0.7576	1.1131	1.0903	0.9490	0.9650	1.0121
1.3	0.6572	0.7338	1.1166	1.0925	0.9495	0.9656	1.0143
1.4	0.6347	0.7106	1.1196	1.0921	0.9497	0.9642	1.0175
1.5	0.6131	0.6866	1.1199	1.0866	0.9503	0.9611	1.0218
1.6	0.5928	0.6613	1.1157	1.0752	0.9524	0.9575	1.0260
1.7	0.5743	0.6352	1.1059	1.0592	0.9565	0.9552	1.0288
1.8	0.5584	0.6095	1.0914	1.0415	0.9625	0.9557	1.0293
1.9	0.5455	0.5860	1.0742	1.0251	0.9697	0.9593	1.0274
2.0	0.5356	0.5659	1.0566	1.0117	0.9773	0.9655	1.0239

Tables 9, 10, 11, 12, 13, 14, 15, and 16 contain the predicted viscosities, diffusion coefficients, and thermal diffusion factors computed by the following relationships.[19]

Viscosity Coefficient.

a) Single Compound

Table 9. The Predicted Transport Properties of an Equimolar Mixture of Ne+O_2 System

T / °K	η / μPa s	D (1.013 bar) / $\times 10^{-4}$ m^2 s^{-1}	α_T
200	18.71	0.1705	0.1159
250	22.23	0.2520	0.1277
300	25.44	0.3452	0.1350
273.15	23.73	0.2935	0.1314
293.15	25.01	0.3316	0.1342
313.15	26.25	0.3717	0.1366
333.15	27.44	0.4130	0.1384
353.15	28.60	0.4561	0.1399
373.15	29.75	0.5011	0.1416
423.15	32.48	0.6202	0.1446
473.15	35.09	0.7492	0.1465
523.15	37.58	0.8873	0.1480
573.15	39.97	1.0343	0.1489
623.15	42.29	1.1907	0.1499
673.15	44.51	1.3546	0.1503
723.15	46.68	1.5273	0.1504
773.15	48.80	1.7086	0.1508
873.15	52.86	2.0934	0.1506
973.15	56.76	2.5100	0.1503
1073.15	60.50	2.9553	0.1495
1173.15	64.13	3.4305	0.1489
1273.15	67.66	3.9338	0.1483
1773.15	84.31	6.8554	0.1466
2273.15	99.85	10.4015	0.1486
2773.15	114.62	14.5092	0.1533
3273.15	128.80	19.1278	0.1595

Table 10. The Predicted Transport Properties of an Equimolar Mixture of Ne+CO_2 System

T / °K	η / μPa s	D (1.013 bar) / $\times 10^{-4}$ m^2 s^{-1}	α_T
250	18.75	0.2006	0.1876
300	21.71	0.2758	0.2024
273.15	20.14	0.2344	0.1953
293.15	21.32	0.2650	0.2008
313.15	22.47	0.2970	0.2054
333.13	23.58	0.3305	0.2099
353.15	24.67	0.3656	0.2138
373.15	25.75	0.4015	0.2168
423.15	28.32	0.4976	0.2233
473.15	30.79	0.6013	0.2283
523.15	33.14	0.7124	0.2322
573.15	35.44	0.8310	0.2354
623.15	37.60	0.9558	0.2377
673.15	39.69	1.0877	0.2398
723.15	41.73	1.2263	0.2414
773.15	43.73	1.3705	0.2425
873.15	47.51	1.6785	0.2443
973.15	51.15	2.0096	0.2451
1073.15	54.60	2.3639	0.2457
1173.15	57.95	2.7405	0.2460
1273.15	61.19	3.1383	0.2457
1773.15	76.22	5.4374	0.2449
2273.15	90.01	8.2126	0.2459
2773.15	102.97	11.4239	0.2500
3273.15	115.28	15.0257	0.2567

Table 11. The Predicted Transport Properties of an Equimolar Mixture of Ne+N_2O System

T / °K	η / μPa s	D (1.013 bar) / $\times 10^{-4}$ m^2 s^{-1}	α_T
300	21.26	0.2737	0.1915
273.15	20.04	0.2322	0.1831
293.15	21.21	0.2628	0.1895
313.15	22.38	0.2952	0.1953
333.15	23.52	0.3289	0.2073
353.15	24.62	0.3637	0.2091
373.15	25.70	0.3999	0.2108
423.15	28.34	0.4964	0.2157
473.15	30.82	0.6005	0.2215
523.15	33.24	0.7123	0.2262
573.15	35.51	0.8310	0.2296
623.15	37.74	0.9571	0.2328
673.15	39.90	1.0895	0.2351
723.15	41.95	1.02284	0.2369
773.15	43.96	1.3740	0.2388
873.15	47.84	1.6834	0.2409
973.15	51.52	2.0170	0.2427
1073.15	55.07	2.3732	0.2435
1173.15	58.45	2.7515	0.2441
1273.15	61.75	3.1522	0.2446
1773.15	76.98	5.4627	0.2438
2273.15	90.87	8.2531	0.2440
2773.15	103.89	11.4860	0.2459
3273.15	116.27	15.1271	0.2498

Table 12. The Predicted Transport Properties of an Equimolar Mixture of Ne+SF_6 System

T / °K	η / μPa s	D (1.013 bar) / $\times 10^{-4}$ m^2 s^{-1}	α_T
250	17.29	0.1217	0.3669
300	20.04	0.1662	0.3865
273.15	18.59	0.1415	0.3766
293.15	19.67	0.1598	0.3841
313.15	20.74	0.1787	0.3905
333.15	21.80	0.1984	0.3956
353.15	22.80	0.2190	0.4002
373.15	23.79	0.2403	0.4044
423.15	26.21	0.2967	0.4132
473.15	28.47	0.3578	0.4204
523.15	30.68	0.4228	0.4252
573.15	32.75	0.4920	0.4296
623.15	34.77	0.5653	0.4330
673.15	36.73	0.6422	0.4357
723.15	38.60	0.7230	0.4380
773.15	40.43	0.8074	0.4399
873.15	43.95	0.9812	0.4420
973.15	47.30	1.1789	0.4436
1073.15	50.52	1.3843	0.4446
1173.15	53.61	1.6026	0.4453
1273.15	56.62	1.8331	0.4462
1773.15	70.56	3.1574	0.4531
2273.15	83.19	4.7411	0.4651
2773.15	94.86	6.5543	0.4800
3273.15	105.75	8.7520	0.4955

Table 13. The Predicted Transport Properties of an Equimolar Mixture of Ar+O_2 System

T / °K	η / μPa s	D (1.013 bar) / $\times 10^{-4}$ m^2 s^{-1}	α_T
200	15.33	0.0935	0.0208
250	18.70	0.1420	0.0284
300	21.81	0.1984	0.0344
273.15	20.18	0.1673	0.0313
293.15	21.40	0.1902	0.0336
313.15	22.60	0.2145	0.0357
333.15	23.77	0.2401	0.0376
353.15	24.89	0.2664	0.0391
373.15	25.98	0.2939	0.0406
423.15	28.62	0.3677	0.0439
473.15	31.10	0.4470	0.0463
523.15	33.48	0.5332	0.0482
573.15	35.73	0.6240	0.0497
623.15	37.90	0.7210	0.0511
673.15	40.01	0.8234	0.0522
723.15	42.03	0.9304	0.0529
773.15	44.01	1.0428	0.0536
873.15	47.80	1.2824	0.0547
973.15	51.42	1.5409	0.0554
1073.15	54.90	1.8181	0.0560
1173.15	58.25	2.1120	0.0563
1273.15	61.51	2.4242	0.0565
1773.15	76.63	4.2284	0.0563
2273.15	90.36	6.4181	0.0553
2773.15	103.18	8.9677	0.0542
3273.15	115.46	11.8628	0.0533

$$\eta = \frac{5}{16}\left(\frac{mkT}{\pi}\right)^{1/2}\frac{f_\eta}{\sigma^2\Omega^{*(2,2)}}, \tag{16}$$

where f_η is the higher order correction factor for the viscosity coefficient that may be defined by

$$f_\eta = 1 + \frac{3}{196}(8E^* - 7)^2, \tag{17}$$

m is the mass of a molecule and E^* is the ratio of collision integrals defined by Eq. 14

b) Mixtures

$$\eta_{mix} = -\frac{\begin{vmatrix} H_{11} & H_{12} & \cdots & H_{1v} & x_1 \\ H_{21} & H_{22} & \cdots & H_{2v} & x_2 \\ \vdots & \vdots & \ddots & \vdots & \vdots \\ H_{v1} & H_{v2} & \cdots & H_{vv} & x_v \\ x_1 & x_2 & \cdots & x_v & 0 \end{vmatrix}}{\begin{vmatrix} H_{11} & H_{12} & \cdots & H_{1v} \\ H_{21} & H_{22} & \cdots & H_{2v} \\ \vdots & \vdots & \ddots & \vdots \\ H_{v1} & H_{v2} & \cdots & H_{vv} \end{vmatrix}}, \tag{18}$$

where,

$$H_{ii} = \frac{x_i^2}{\eta_i} + \sum_{\substack{k=1 \\ k\neq i}}^{v} \frac{2x_ix_k}{\eta_{ik}}\frac{m_im_k}{(m_k+m_i)^2}\left(\frac{5}{3A_{ik}^*} + \frac{m_k}{m_i}\right), \tag{19}$$

Table 14. The Predicted Transport Properties of an Equimolar Mixture of Ar+CO_2 System

T / °K	η / μPa s	D (1.013 bar) / $\times 10^{-4}$ m^2 s^{-1}	α_T
250	15.70	0.1032	0.0146
300	18.57	0.1459	0.0193
273.15	17.04	0.1222	0.0169
293.15	18.19	0.1398	0.0187
313.15	19.28	0.1580	0.0205
333.15	20.36	0.1773	0.0222
353.15	21.44	0.1978	0.0237
373.15	22.48	0.2190	0.0251
423.15	24.96	0.2753	0.0280
473.15	27.35	0.3371	0.0304
523.15	29.59	0.4032	0.0323
573.15	31.81	0.4748	0.0339
623.15	34.01	0.5495	0.0351
673.15	35.85	0.6292	0.0362
723.15	37.65	0.7135	0.0372
773.15	39.69	0.8006	0.0378
873.15	43.29	0.9874	0.0391
973.15	46.72	1.1890	0.0399
1073.15	49.99	1.4047	0.0406
1173.15	53.17	1.6349	0.0412
1273.15	56.21	1.8770	0.0416
1773.15	70.30	3.2794	0.0430
2273.15	82.97	4.9711	0.0437
2773.15	94.63	6.9303	0.0441
3273.15	105.66	9.1432	0.0443

$$H_{ij}(i\neq j) = -\frac{2x_ix_j}{\eta_{ij}}\frac{m_im_j}{(m_i+m_j)^2}\left(\frac{5}{3A_{ik}^*} - 1\right), \tag{20}$$

$$\eta_{ij} = \frac{5}{16}\left[\left(\frac{2m_im_j}{m_i+m_j}\right)\frac{kT}{\pi}\right]^{1/2}\frac{1}{\sigma_{ij}^2\Omega_{ij}^{*(2,2)}(T_{ij}^*)}, \tag{21}$$

A_{ij}^* is the ratio of the collision integrals [Eq. 11], x is the mole fraction of components, and η_{ij} is the interaction viscosity. Subscript i represents the heavier component and subscript j represents the lighter component of the i–j pair.

Diffusion Coefficient.

Diffusion in multicomponent mixtures is entirely described in terms of the binary diffusion coefficients, D_{ij},

$$D_{ij} = \frac{3}{8}\left[\left(\frac{m_i+m_j}{2m_im_j}\right)\frac{kT}{\pi}\right]^{1/2}\frac{kT}{P}\frac{1+\Delta_{ij}}{\sigma_{ij}^2\Omega_{ij}^{*(1,1)}(T_{ij}^*)}, \tag{22}$$

where P is the pressure and Δ_{ij} is a higher order correction term of the binary diffusion coefficient, which can be defined as

$$\Delta_{ij} \approx 1.3(6C_{ij}^* - 5)^2\frac{a_{ij}x_{ij}}{1+b_{ij}x_{ij}}, \tag{23}$$

where

$$a_{ij} = \frac{\sqrt{2}}{8[1+1.8(m_j/m_i)]^2}\frac{\Omega_{ij}^{*(1,1)}(T_{ij}^*)}{\Omega_{jj}^{*(2,2)}(T_j^*)},$$

Table 15. The Predicted Transport Properties of an Equimolar Mixture of Ar+N_2O System

T / °K	η / μPa s	D (1.013 bar) / $\times 10^{-4}$ m^2 s^{-1}	α_T
300	18.60	0.1466	0.0185
273.15	17.06	0.1225	0.0161
293.15	18.28	0.1413	0.0184
313.15	19.32	0.1588	0.0196
333.15	20.42	0.1781	0.0212
353.15	21.49	0.1986	0.0228
373.15	22.55	0.2202	0.0242
423.15	25.07	0.2769	0.0270
473.15	27.49	0.3396	0.0295
523.15	29.78	0.4062	0.0312
573.15	31.98	0.4782	0.0329
623.15	34.10	0.5545	0.0341
673.15	36.14	0.6345	0.0351
723.15	38.11	0.7194	0.0361
773.15	40.03	0.8084	0.0368
873.15	43.69	0.9969	0.0379
973.15	47.18	1.2016	0.0389
1073.15	50.52	1.4193	0.0394
1173.15	53.73	1.6522	0.0401
1273.15	56.83	1.8975	0.0405
1773.15	71.13	3.3155	0.0418
2273.15	83.98	5.0263	0.0426
2773.15	95.81	7.0074	0.0430
3273.15	106.98	9.2458	0.0432

$$b_{ij} = 10a_{ij}\left[1 + 1.8(m_j/m_i) + 3(m_j/m_i)^2\right] - 1, \quad (24)$$

$$x_{ij} = \frac{x_i}{x_i + x_j}.$$

Note that all units are in the SI system.

Thermal Diffusion Factor. An expression for the thermal-diffusion factor of a binary mixture is:

$$\alpha_T = (6C_{ij}^* - 5)\left(\frac{x_1S_1 - x_2S_2}{x_1^2Q_1 + x_2^2Q_2 + x_1x_2Q_{12}}\right)(1 + k_T), \quad (25)$$

where k_T is a higher order correction term for the thermal-diffusion factor. This term is usually negligible compared with experimental uncertainties in α_T. The other quantities in Eq. 25 are:

$$S_1 = \frac{m_1}{m_2}\left(\frac{2m_2}{m_1+m_2}\right)^{1/2}\frac{\sigma_{11}^2\Omega_{11}^{*(2,2)}(T_1^*)}{\sigma_{12}^2\Omega_{12}^{*(1,1)}(T_{12}^*)} - \frac{4m_1m_2A_{12}^*}{(m_1+m_2)^2} + \frac{15m_2(m_1-m_2)}{2(m_1+m_2)^2}, \quad (26)$$

$$Q_1 = \frac{2}{m_2(m_1+m_2)}\left(\frac{2m_2}{m_1+m_2}\right)^{1/2}\frac{\sigma_{11}^2\Omega_{11}^{*(2,2)}(T_1^*)}{\sigma_{12}^2\Omega_{12}^{*(1,1)}(T_{12}^*)}\left[\left(\frac{5}{2} - \frac{6}{5}B_{12}^*\right)m_1^2 + 3m_2^2 + \frac{8}{5}m_1m_2A_{12}^*\right], \quad (27)$$

$$Q_{12} = 15\left(\frac{m_1-m_2}{m_1+m_2}\right)^2\left(\frac{5}{2} - \frac{6}{5}B_{12}^*\right) + \frac{4m_1m_2A_{12}^*}{(m_1+m_2)^2}\left(11 - \frac{12}{5}B_{12}^*\right) + \frac{8}{5}\frac{(m_1+m_2)\sigma_{11}^2\Omega_{11}^{*(2,2)}(T_1^*)\sigma_{22}^2\Omega_{22}^{*(2,2)}(T_2^*)}{(m_1m_2)^{1/2}\sigma_{12}^2\Omega_{12}^{*(1,1)}(T_{12}^*)\sigma_{12}^2\Omega_{12}^{*(1,1)}(T_{12}^*)}. \quad (28)$$

Table 16. The Predicted Transport Properties of an Equimolar Mixture of Ar+SF_6 System

T / °K	η / μPa s	D (1.013 bar) / $\times 10^{-4}$ m^2 s^{-1}	α_T
250	15.45	0.0625	0.1666
300	18.16	0.0876	0.1765
273.15	16.75	0.0738	0.1603
293.15	17.80	0.0840	0.1727
313.15	18.85	0.0948	0.1841
333.15	19.90	0.1062	0.1946
353.15	20.89	0.1180	0.2043
373.15	21.85	0.1302	0.2128
423.15	24.22	0.1632	0.2315
473.15	26.43	0.1987	0.2463
523.15	28.58	0.2371	0.2585
573.15	30.60	0.2781	0.2686
623.15	32.56	0.3213	0.2770
673.15	34.47	0.3673	0.2846
723.15	36.28	0.4153	0.2906
773.15	38.05	0.4654	0.2956
873.13	41.48	0.5729	0.3048
973.15	44.71	0.6879	0.3113
1073.15	47.84	0.8115	0.3169
1173.15	50.28	0.9423	0.3211
1273.15	53.72	1.0806	0.3245
1773.15	67.02	1.8771	0.3361
2273.15	78.89	2.8320	0.3406
2773.15	89.78	3.9343	0.3426
3273.15	99.99	5.1734	0.3437

The expression for S_2 and Q_2 are obtained from those of S_1 and Q_1 by interchanging subscript 1 and 2. The sign convention for α_T requires that subscript 1 denotes the heavier component. It must be mentioned that another interesting advantage of the inversion procedure, in this work, is that one can evaluate the transport properties for temperatures, which may not be experimentally available. By this we mean that the transport properties can be determined for higher temperature than that cited in this paper; however, we have confined ourselves to use temperatures from 200 to 3273.15 °K.

It should be mentioned that this paper concerns molecular gases rather than just binary noble gases or CH_4 (nearly noble gases) +noble gases, like the previous ones. It comes as somewhat of a surprise that a spherical potential serves for a wide variety of molecular gases (O_2, N_2O, CO_2, and SF_6) with sufficient accuracy for our purposes.

The diffusion coefficients depend almost entirely on the unlike interactions in the mixture, and are influenced by the like interactions to the extent of a few percent, at most. They therefore supply a more direct test of the combination rules than do mixture viscosities, but unfortunately the experimental accuracy of the measurements is distinctly lower than in

the case of the viscosity. Scatter in the data as high as ±10% can be seen to be not uncommon (Tables 17 and 18). The calculated values of α_T may well involve uncertainties that are about one order of magnitude (about factor of 10) larger than the corresponding uncertainties in η_{mix} and D_{12}. The saving grace is that the measured values of α_T also involve uncertainties of similar magnitude.

Concluding Remarks. The direct inversion of the viscosity collision integral correlations obtained from an extended law of the corresponding states is obviously a powerful method for establishing an accurate unlike-pair potential energy. It is an advancement over the traditional approaches that consider a potential function with several parameters and to try to adjust them using experimental results. The intermolecular potential energy of Ar+SF_6 from the inversion method has been well compared with that of Taylor et al.[14] It is of interest to mention that the potential energy obtained by the inversion procedure could produce, within the experimental accuracy, transport properties. Our estimated accuracies are within 1% for η (viscosity), 5% for D_{12} (binary diffusion coefficient), and 25% for α_T (thermal diffusion factor).

These accuracies are comparable to, but somewhat poorer than, the corresponding estimated accuracies for the pure components reported in Ref. 24. They are poorer than the corresponding accuracies for the noble-gas mixtures reported in Ref. 18, but enjoy the advantage of operation in an entirely predictive mode. For a precise estimate of particular mixtures, it is necessary to examine the experimental data in detail.

It should be mentioned that the recently determined scaling parameters for polyatomic gases by Bzowski et al.[19] exhibit a discrepancy by a factor 0.997 in the distance of zero potential.

Table 17. Deviation of the Calculated Values of the Diffusion Coefficients of Mixtures from the Experimental Values

Ar+O_2[a]						
T (K)	298.15	368.15	468.15	576.15	667.15	770.15
D_{Exp}	0.1950	0.2890	0.4410	0.6280	0.8070	1.0360
D_{Calc}	0.1961	0.2869	0.4388	0.6296	0.8110	1.0358
Dev%[b]	−0.56	0.73	0.50	−0.25	−0.49	0.02
Ar+CO_2[c]						
T (K)		293.15			303.15	
D_{Exp}		0.1430			0.1530	
D_{Calc}		0.1398			0.1488	
Dev%[b]		2.29			2.82	
Ar+SF_6[d]						
T (K)	298.15	333.15	378.15	423.15	473.15	
D_{Exp}	0.0827	0.0998	0.1300	0.1580	0.2010	
D_{Calc}	0.0866	0.1062	0.1334	0.1632	0.1987	
Dev%[b]	−4.50	−6.96	−2.55	−3.19	1.16	
Ne+O_2[d]						
T (K)	298.15	378.15	478.15	573.15	678.15	
D_{Exp}	0.3190	0.4930	0.7420	1.0000	1.3400	
D_{Calc}	0.3370	0.5060	0.7527	1.0265	1.3537	
Dev%[b]	−5.30	−2.60	−1.40	−2.60	−1.00	
Ne+CO_2[e]						
T (K)		293.15			303.15	
D_{Exp}		0.2510			0.2670	
D_{Calc}		0.2615			0.2771	
Dev%[b]		−4.00			−3.60	
Ne+SF_6[d]						
T (K)	298.15	328.15	378.15	423.15	483.15	
D_{Exp}	0.1550	0.1860	0.2380	0.2890	0.3630	
D_{Calc}	0.1623	0.1909	0.2426	0.2929	0.3657	
Dev%[b]	−4.50	−2.60	−1.90	−1.30	−0.70	

a) Ref. 25. b) $\text{Dev\%} = \frac{D_{Exp}-D_{Calc}}{D_{Calc}} \times 100$. c) Ref. 26. d) Ref. 27. e) Ref. 28.

Table 18. Deviation of the Calculated Values of the Thermal Diffusion Factor of Mixtures from the Experimental Values

				$Ne+CO_2$				
T (K)=342.9[a]								
X_{Ne}	0.021	0.176	0.302	0.430	0.570	0.710	0.837	0.927
$(\alpha_T)_{Exp}$	0.1620	0.1730	0.1930	0.2200	0.2290	0.2410	0.2900	0.3380
$(\alpha_T)_{Calc}$	0.1583	0.1725	0.1859	0.2019	0.2227	0.2481	0.2766	0.3008
Dev%[b]	2.34	0.29	3.82	8.96	2.83	−2.86	4.84	12.37
T (K)=269.8[c]								
X_{CO_2}	0.190	0.199	0.210	0.795	0.805	0.815		
$(\alpha_T)_{Exp}$	0.1900	0.1920	—	0.1230	0.1220	—		
$(\alpha_T)_{Calc}$	0.2483	0.2463	0.2440	0.1605	0.1595	0.1586		
Dev%[b]	−23.48	−22.05	—	−23.36	−23.50	—		
T (K)=300[c]								
X_{CO_2}	0.190	0.199	0.210	0.795	0.805	0.815		
$(\alpha_T)_{Exp}$	0.2020	—	0.1980	0.1290	—	0.1270		
$(\alpha_T)_{Calc}$	0.2583	0.2562	0.2538	0.1673	0.1664	0.1654		
Dev%[b]	−21.80	—	−22.00	−22.89	—	−23.22		
T (K)=323.7[c]								
X_{CO_2}	0.190	0.199	0.210	0.795	0.805	0.815		
$(\alpha_T)_{Exp}$	—	0.2050	0.2040	—	0.1320	0.1310		
$(\alpha_T)_{Calc}$	0.2651	0.2630	0.2605	0.1720	0.1710	0.1700		
Dev%[b]	—	−22.05	−21.69	—	−22.81	−22.94		
				$Ne+SF_6$[d]				
T (K)=255.3								
X_{SF_6}	0.19	0.21	0.79	0.81				
$(\alpha_T)_{Exp}$	0.4650	0.4410	0.2320	0.2270				
$(\alpha_T)_{Calc}$	0.5883	0.5667	0.2751	0.2703				
Dev%[b]	−20.96	−22.18	−15.67	−16.02				
T (K)=300								
X_{SF_6}	0.18	0.20	0.80					
$(\alpha_T)_{Exp}$	0.508	0.480	0.246					
$(\alpha_T)_{Calc}$	0.6261	0.6027	0.2848					
Dev%[b]	−18.86	−20.36	−13.62					

a) Ref. 29. b) $\text{Dev}\% = \frac{(\alpha_T)_{Exp}-(\alpha_T)_{Calc}}{(\alpha_T)_{calc}} \times 100$. c) Ref. 30. d) Ref. 31.

The authors wish to thank the Computer Center and the Department of Chemistry of Shiraz University for the Computer facilities. One of us (M. M Papari) thanks S. Papari for her helpful assistance. The authors are also indebted to the Research Committee of Shiraz University.

References

1) J. A. Barker, R. O. Watts, J. K. Lee, T. P. Schafer, and Y. T. Lee, *J. Chem. Phys.*, **61**, 3081 (1974).
2) D. W. Gough, G. C. Maitland, and E. B. Smith, *Mol. Phys.*, **24**, 151 (1972).
3) G. C. Maitland and E. B. Smith, *Mol. Phys.*, **24**, 1185 (1972).
4) G. C. Maitland and E. B. Smith, *Chem. Soc. Rev.*, **2**, 181 (1973).
5) A. Boushehri, L. A. Viehland, and E. A. Mason, *Chem. Phys.*, **28**, 313 (1978).
6) A. Boushehri, *Physica A*, **97A**, 206 (1979).
7) A. Boushehri and J. M. Absardi, *Bull. Chem. Soc. Jpn.*, **62**, 1313 (1989).
8) A. Boushehri and A. Maghari, *J. Phys. Soc. Jpn.*, **59**, 4302 (1990).
9) E. K. Goharshadi and A. Boushehri, *Bull. Chem. Soc. Jpn.*, **67**, 2403 (1994).
10) A. Boushehri and M. H. Mousazadeh, *J. Phys. Soc. Jpn.*, **64**, 331 (1995).
11) A. Boushehri and F. S. Hashemi, *Bull. Chem. Soc. Jpn.*, **69**, 67 (1996).
12) M. H. Ghatee, M. M. Papari, and A. Boushehri, *Bull. Chem. Soc. Jpn.*, **70**, 2643 (1997).
13) J. O. Hirschfelder, C. F. Curtiss, and R. B. Bird, "Molecular Theory of Gases and Liquids," John Wiley, New York (1954).
14) W. L. Taylor and J. J. Hurly, *J. Chem. Phys.*, **98**, 2291 (1993).
15) J. Kestin, S. T. Ro, and W. A. Wakeham, *J. Chem. Phys.*, **36**, 4119 (1972).
16) Y. Abe, J. Kestin, H. E. Khalifa, and W. A. Wakeham, *Physica A*, **93A**, 155 (1978).
17) Y. Abe, J. Kestin, H. E. Khalifa, and W. A. Wakeham, *Ber. Bungsenges. Phys. Chem.*, **83**, 271 (1979).
18) B. Najafi, E. A. Mason and J. Kestin, *Physica A*, **119A**, 387 (1983).
19) J. Bzowski, J. Kestin, E. A. Mason, and F. J. Uribe, *J. Phys. Chem. Ref. Data*, **19**, 1179 (1990).
20) L. A. Viehland, E. A. Mason, W. F. Morrison, and M. R.

Flannery, *At. Data Nucl. Data Tables*, **16**, 495 (1975).
21) H. O'Hara and F. J. Smith, *J. Comput. Phys.*, **5**, 328 (1970).
22) H. O'Hara and F. J. Smith, *Comput. Phys. Commun.*, **2**, 47 (1971).
23) G. C. Maitland, E. A. Mason, L. A. Viehland, and W. A. Wakeham, *Mol. Phys.*, **36**, 797 (1978).
24) A. Boushehri, J. Bzowski, J. Kestin, and E. A. Mason, *J. Phys. Chem. Ref. Data*, **16**, 445 (1987).
25) J. M. Hellemans, J. Kestin, and S. T. Ro, *Physica*, **65**, 362 (1973).
26) J. Kestin, Y. Kobayashi, and R. T. Wood, *Physica*, **32**, 1065 (1966).
27) J. Kestin, H. E. Khalifa, S. T. Ro, and W. A. Wakeham, *Physica A*, **88A**, 242 (1977).
28) J. D. Breetveld, R. Dipippo, and J. Kestin, *J. Chem. Phys.*, **45**, 124 (1966).
29) A. K. Batabyal and A. K. Barua, *J. Chem. Phys.*, **48**, 2557 (1968).
30) R. D. Trengove and P. J. Dunlop, *Chem. Phys. Lett.*, **94**, 118 (1983).
31) R. D. Trengove, H. L. Robjohns, and P. J. Dunlop, *Physica A*, **128A**, 486 (1984).